Author/s:
Syeda, WT;Wannan, CMJ;Merritt, AH;Raghava, JM;Jayaram, M;Velakoulis, D;Kristensen, TD;Soldatos, RF;Tonissen, S;Thomas, N;Ambrosen, KS;Sørensen, ME;Fagerlund, B;Rostrup, E;Glenthøj, BY;Skafidas, E;Bousman, CA;Johnston, LA;Everall, I;Ebdrup, BH;Pantelis, C

Title:
Cortico-cognition coupling in treatment resistant schizophrenia

Date:
2022-01-01

Citation:
Syeda, W. T., Wannan, C. M. J., Merritt, A. H., Raghava, J. M., Jayaram, M., Velakoulis, D., Kristensen, T. D., Soldatos, R. F., Tonissen, S., Thomas, N., Ambrosen, K. S., Sørensen, M. E., Fagerlund, B., Rostrup, E., Glenthøj, B. Y., Skafidas, E., Bousman, C. A., Johnston, L. A., Everall, I. ,... Pantelis, C. (2022). Cortico-cognition coupling in treatment resistant schizophrenia. Neuroimage Clinical, 35, https://doi.org/10.1016/j.nicl.2022.103064.

Persistent Link:
https://hdl.handle.net/11343/316206

NeuroImage: Clinical 35 (2022) 103064

Contents lists available at ScienceDirect

NeuroImage: Clinical

journal homepage: www.elsevier.com/locate/ynicl

Cortico-cognition coupling in treatment resistant schizophrenia

Warda T. Syeda [a,1,*], Cassandra M.J. Wannan [a,1], Antonia H. Merritt [a], Jayachandra M. Raghava [b,e], Mahesh Jayaram [a,d], Dennis Velakoulis [a], Tina D. Kristensen [b], Rigas Filippos Soldatos [a,h], Shane Tonissen [a], Naveen Thomas [a,d], Karen S. Ambrosen [b], Mikkel E. Sørensen [b], Birgitte Fagerlund [b], Egill Rostrup [b], Birte Y. Glenthøj [b,c], Efstratios Skafidas [a], Chad A. Bousman [a,f], Leigh A. Johnston [i], Ian Everall [g], Bjørn H. Ebdrup [a,b,c,1], Christos Pantelis [a,b,d,j,1]

[a] Melbourne Neuropsychiatry Centre, Department of Psychiatry, University of Melbourne and Melbourne Health, Victoria, Australia
[b] Center for Neuropsychiatric Schizophrenia Research and Center for Clinical Intervention and Neuropsychiatric Schizophrenia Research, Mental Health Centre Glostrup, University of Copenhagen, Glostrup, Denmark
[c] Faculty of Health and Medical Sciences, Department of Clinical Medicine, University of Copenhagen, Copenhagen, Denmark
[d] MidWest Area Mental Health Service, Sunshine Hospital, St. Albans, Victoria, Australia
[e] Functional Imaging Unit, Department of Clinical Physiology, Nuclear Medicine and PET, Rigshospitalet, Glostrup, Denmark
[f] Departments of Medical Genetics, Psychiatry, and Physiology & Pharmacology, University of Calgary, Canada
[g] Institute of Psychiatry, Psychology and Neuroscience, King's College London, UK
[h] First Department of Psychiatry, National and Kapodistrian University of Athens Medical School, Eginition Hospital, Athens, Greece
[i] Department of Biomedical Engineering and Melbourne Brain Centre Imaging Unit, University of Melbourne, Victoria, Australia
[j] The Florey Institute of Neuroscience and Mental Health, Victoria, Australia

ARTICLE INFO

Keywords:
Partial least squares correlation
Treatment-resistant schizophrenia
Cognition
Brain structure
MRI

ABSTRACT

Background: Brain structural alterations and cognitive dysfunction are independent predictors for poor clinical outcome in schizophrenia, and the associations between these domains remains unclear. We employed a novel, multiblock partial least squares correlation (MB-PLS-C) technique and investigated multivariate cortico-cognitive patterns in patients with treatment-resistant schizophrenia (TRS) and matched healthy controls (HC).

Method: Forty-one TRS patients (age 38.5 ± 9.1, 30 males (M)), and 45 HC (age 40.2 ± 10.6, 29 M) underwent 3T structural MRI. Volumes of 68 brain regions and seven variables from CANTAB covering memory and executive domains were included. Univariate group differences were assessed, followed by the MB-PLS-C analyses to identify group-specific multivariate patterns of cortico-cognitive coupling. Supplementary three-group analyses, which included 23 non-affected first-degree relatives (NAR), were also conducted.

Results: Univariate tests demonstrated that TRS patients showed impairments in all seven cognitive tasks and volume reductions in 12 cortical regions following Bonferroni correction. The MB-PLS-C analyses revealed two significant latent variables (LVs) explaining > 90% of the sum-of-squares variance. LV1 explained 78.86% of the sum-of-squares variance, describing a shared, widespread structure-cognitive pattern relevant to both TRS patients and HCs. In contrast, LV2 (13.47% of sum-of-squares variance explained) appeared specific to TRS and comprised a differential cortico-cognitive pattern including frontal and temporal lobes as well as paired associates learning (PAL) and intra-extra dimensional set shifting (IED). Three-group analyses also identified two significant LVs, with NARs more closely resembling healthy controls than TRS patients.

Abbreviations: MB-PLS-C, Multiblock Partial Least Squares Correlation; PAL, Paired Associates Learning; IED, Intra-extra Dimensional Set Shifting; LV, Latent Variable; TRS, Treatment Resistant Schizophrenia; BMI, Body Mass Index; HC, Healthy Control; NAR, Non-affected Relatives; M.I.N.I., Mini International Neuropsychiatric Interview; PANSS, Positive and Negative Syndrome Scale; GAF, Global Assessment of Functioning; SOFAS, Social and Occupational Functioning Assessment Scale; WTAR, Wechsler Test of Adult Reading; CANTAB, Cambridge Neuropsychological Test Automated Battery; MPRAGE, Magnetization-Prepared Rapid Acquisition Gradient Echo; SSP, Spatial Span; SWM, Spatial Working Memory; TIV, Total Intracranial Volume; NSSD, Normalized Structure Salience Difference.

* Corresponding author.
E-mail address: wtsyeda@unimelb.edu.au (W.T. Syeda).
[1] These authors contributed equally to this work.

https://doi.org/10.1016/j.nicl.2022.103064
Received 27 January 2022; Received in revised form 10 May 2022; Accepted 26 May 2022
Available online 28 May 2022

Conclusions: MB-PLS-C analyses identified multivariate brain structural-cognitive patterns in the latent space that may provide a TRS signature.

1. Introduction

Schizophrenia is a heritable psychiatric disorder (Hilker et al., 2018) characterized by positive and negative symptoms, as well as broad cognitive dysfunction and abnormalities in brain structure and function (Kochunov et al., 2020; van Erp et al., 2018). Recent modelling suggests that around 22% of schizophrenia patients do not respond adequately to antipsychotic treatment and are considered treatment resistant (TRS) (Mørup et al., 2020). Clozapine is the treatment of choice for those with TRS, however, only about 40% of those on clozapine respond well, leading to an 11-fold higher burden of disease in those with TRS compared to responders (Nucifora et al., 2019). Across the schizophrenia-spectrum, the most profound cognitive and brain structural deficits are observed in patients with TRS (Spangaro et al., 2021; Wannan et al., 2019). Given that cognitive impairments are one of the strongest predictors of functional disability in schizophrenia (Bowie and Harvey, 2006), identifying differential patterns of brain structure-cognition relationships in TRS compared to healthy controls is an important step towards identifying TRS-specific mechanisms or treatment targets for cognitive impairments.

For several decades, schizophrenia research has attempted to understand relationships between cognitive deficits and brain structural abnormalities. While localised brain abnormalities have been linked to specific cognitive deficits (Karantonis et al., 2021), it is less clear how patterns of interrelated cognitive dysfunctions map onto distributed patterns of structural brain abnormalities - particularly in less frequently studied populations such as TRS. One method for investigating patterns of relationships between variables is partial least squares correlations analysis (PLS-C): a statistical method which integrates information from multiple data blocks into a single multivariate model (Krishnan et al., 2011; Van Roon et al., 2014). The PLS-C technique identifies latent patterns of associations across multimodal data (e.g., neuroimaging, cognitive, and clinical measures) and between experimental groups.

Recent studies have applied PLS-C techniques in both first-episode and chronic schizophrenia populations. In antipsychotic-naive, first-episode schizophrenia, differential patterns of brain structure-cognition relationships were observed in patients versus healthy controls (Jessen et al., 2019). In chronic schizophrenia, cognitive deficits were found to map onto a network of brain regions centered on the default mode and visual networks (Kirschner et al., 2020). These studies highlight the utility of PLS-C for identifying patterns of brain structure-cognition relationships in psychiatric disorders. However, conventional application of PLS-C on clinical data is typically limited to testing two groups and renders challenges regarding interpretability because of difficulties in 'back translating' the identified latent patterns to a few specific input variables. Also, the effects of covariates are not modelled by conventional PLS-C and it is a standard practice in PLS-C research to control for covariates, either through residualisation (Jessen et al., 2019; Xu et al., 2003) or in post hoc analyses with covariates residing in the native space (Xu et al., 2003).

We here apply our recently developed extended multiblock PLS-C method (MB-PLS-C), which extends the PLS-C model to enable covariate representation in the latent space, along with an integrated interpretation framework (Syeda et al., 2021). The proposed method enables 1) covariate blocks for each modality of interest, 2) decomposition of the input correlation matrix into additive components to aid with interpretation of the latent variables (LVs), 3) calculation of a new metric denoted as normalized structure salience difference (NSSD) to evaluate between-group differences in salience strengths, and 4) between-group comparisons for ≥ 2 groups.

In this study of patients with treatment-resistant schizophrenia (TRS) as well as age- and sex-matched healthy controls (HCs) we first tested for unimodal group differences in brain volumes across 68 predefined regions, and in seven cognitive tasks covering memory and executive domains. Next, we employed our multiblock partial least squares correlation (MB-PLS-C) technique to tease out brain structural-cognitive patterns, which are discriminatory of TRS. Finally, to explore the heritable component of these brain structure-cognition relationships, we conducted 3-group MB-PLS-C analyses with the inclusion of a smaller group of non-affected, first-degree relatives (NAR).

2. Methods

2.1. Participants

The study was approved by the Melbourne Health Human Research Ethics Committee (MHREC ID 2012.069). All participants provided written informed consent prior to inclusion. Ninety-six individuals with TRS were recruited from inpatient and outpatient clinics in Melbourne, Australia between 2012 and 2018. TRS participants were resistant to antipsychotic treatment, defined as no prior response to at least two antipsychotics of two different chemical classes for at least six weeks each at dosages equivalent to $\geq$ 400 mg/d chlorpromazine, and having either been prescribed or treated with clozapine at the time of assessment (Kane et al., 1988; Suzuki et al., 2012). Inclusion criteria included a diagnosis of schizophrenia as verified by the Mini International Neuropsychiatric Interview (M.I.N.I.) (Lecrubier et al., 1997), aged 18–65 years, and undergoing clozapine treatment.

Healthy control participants (n = 67) were frequency matched for age and sex with TRS participants. They were recruited from the general community, and exclusion criteria included (1) previous or current history of psychiatric, neurological disorders or substance abuse or dependence, (2) prior or current use of antipsychotic medication, (3) premorbid IQ $<$ 70, (4) impaired thyroid function, or (5) history of significant head injury and seizures. The M.I.N.I. was used to rule out current or past psychopathology in healthy controls (Lecrubier et al., 1997). Thirty-eight non-affected, first-degree relatives (NAR) (siblings or parents) were initially identified through the participants with schizophrenia and then approached for consent and participation. Participants with at least one missing variable-of-interest were excluded, resulting in a final sample of 45 HCs, 41 TRS and 23 NAR participants.

2.2. Clinical assessment

Clinical symptom severity was assessed using the Positive and Negative Syndrome Scale (PANSS) (Kay et al., 1987), with social and occupational functioning measured with the Global Assessment of Functioning (GAF) (Hall et al.,1995) and the Social and Occupational Functioning Assessment Scale (SOFAS) (Goldman et al., 1992).

2.3. Cognitive/behaviour assessment

Premorbid IQ was assessed with the Wechsler Test of Adult Reading (WTAR) (Holdnack et al., 2001). A total of seven CANTAB metrics assessing memory and executive function were selected pre-hoc based on the opinion of two experts (CP and BF) and previous studies (Wannan et al., 2019; Jessen et al., 2019; Pantelis et al., 2009) (Table 1).

Table 1
CANTAB and premorbid cognitive metrics.

Cognitive test	Cognitive variable	Cognitive functions assessed
Premorbid intelligence	Weschler test of adult reading - UK (WTAR-UK)	Intellectual function prior to illness onset
Paired Associates Learning (PAL)	Total errors (PAL-TE)	Visual memory, new learning
	Stages completed (PAL-SC)*	
Intra-Extra Dimensional Set Shift (IED)	Interdimensional shift (IED-IS)	Visual discrimination, flexibility of attention
	Extradimensional shift (IED-ES)	
Spatial span length (SSP-SL)	Spatial span length (SSP-SL)*	Visuospatial working memory
Spatial working memory (SWM)	Strategy (SWM-S)	Executive function, strategy, working memory
	Total errors (SWM-TE)	

* These variables are recomputed as max(V)-V, where V is the variable of interest to ensure intuitive comparability with other cognitive variables, where a smaller value describes better cognitive performance.

2.4. MRI acquisition

T_1-weighted magnetic resonance images were acquired using an optimized Magnetization-Prepared Rapid Acquisition Gradient Echo (MPRAGE) sequence on a Siemens Avanto 3T Magnetom TIM Trio scanner. The acquisition parameters and image processing protocol are presented in the *Supplementary Material*. Briefly, images were processed using FreeSurfer version 6.0 (https://surfer.nmr.mgh.harvard.edu) to segment gray-white matter tissue (Fischl et al., 2004). The cortical surface was parcellated into 68 regions (Desikan-Killiany atlas), (Desikan et al., 2006) and cortical volume, surface area, and thickness estimates were computed.

3. Statistical analyses

Univariate between-group differences in the demographic, clinical, cognitive and cortical variables were assessed using an appropriate statistical test depending on the distribution of the data (see *Supplementary Material* for details).

3.1. Multiblock partial least squares correlation analyses

A two-group extended MB-PLS-C framework was employed to investigate the latent relationships between brain structure and cognitive measures in TRS and HC cohorts (Syeda et al., 2021). MB-PLS-C identifies multivariate patterns of maximal covariance between disjoint data-blocks, each consisting of multiple variables and observations from the same experimental groups. Mathematical formulation of MB-PLS-C has been presented in the *Supplementary Material*. Briefly, MB-PLS-C was employed to determine the combined patterns of association between four training data blocks (n = 30 per group, see *Supplementary Material* for more details): cognition block, $\boldsymbol{X}$, cortical block, $\boldsymbol{Y}$, cognition covariate block, $\boldsymbol{C_X}$ and cortical covariate block $\boldsymbol{C_Y}$. Data block $\boldsymbol{X}$ was constructed from the cognitive variables in Table 1, and $\boldsymbol{C_X}$ contained age, sex and premorbid-IQ. Similarly, data block $\boldsymbol{Y}$ was constructed from regional cortical volumes. The cortical covariate block $\boldsymbol{C_Y}$ included age, sex, BMI and total intracranial volume, which have all been associated with cortical volumes. Group-specific block cross-correlation matrices were constructed and combined to form a single cross-correlation matrix, $\boldsymbol{R}$, which was decomposed into latent components using singular value decomposition. The latent components described a pattern of features or *saliences* in cortical, cognitive, and covariate domains.

To establish statistical validity of the patterns arising from MB-PLS-C, a number of non-parametric tests were employed including: 1) permutation testing to assess statistical significance, 2) bootstrapping to estimate salience-specific confidence intervals, 3) cross-validation to assess generalizability of the MB-PLS-C model (LV-specific cortico-cognitive correlation coefficient) (Kirschner et al., 2020). Further description of these tests is presented in the *Supplementary Material*.

Finally, a three-group extended MB-PLS-C framework was implemented by extending the four data-blocks, $\boldsymbol{X}$, $\boldsymbol{Y}$, $\boldsymbol{C_X}$, $\boldsymbol{C_Y}$, to include NAR participants, followed by construction of the cross-correlation matrix, $\boldsymbol{R}$, singular value decomposition and statistical testing.

3.2. Interpretation of cortical and cognitive saliences

The LV-specific patterns of cortical volume and cognitive saliences describe contributions of individual cortical volume and cognitive variables to their respective latent variables (see Eqs S1-S3 in the *Supplementary Material*). Cortical volume saliences describe group-wise patterns where, for each cortical volume variable, the polarity of the between-group saliences indicated their relationship, i.e., saliences with same polarity showed a shared pattern and saliences with opposite polarity described a differential pattern across groups. On the other hand, the cognitive saliences described an overall pattern with averaged contributions from all groups.

The strength of cortico-cognition coupling between a cortical volume salience and a cognitive salience is characterized by their product (Eq S3), with a larger value of the product indicating stronger cortico-cognitive associations and the polarity of the product indicating the direction of the association.

3.3. Normalized between-group structural salience difference (NSSD)

The cortical latent variables are the weighted linear combination of cortical volumes, with the weights defined by the group-wise structural pattern of cortical saliences. To assess group differences in the cortical patterns between healthy controls and TRS patients, a normalized measure of between-group structure salience difference (NSSD) for the i th LV and j th cortical volume variable is defined as:

$$\kappa_{ij} = \frac{|u_{ij,HC}| - |u_{ij,TRS}|}{s_{pool}},$$

where $|x|$ is the absolute value. $u_{ij,HC}$ and $u_{ij,TRS}$ are the j th cortical saliences of the HC and TRS groups for the i th LV, respectively. s_{pool} is the pooled expected variation in the salience strengths calculated from combined confidence intervals: $s_g = u^{LL}_{ij,g} + u^{UL}_{ij,g}, g \in \{HC, TRS\}$, where $u^{LL}_{ij,g}, u^{UL}_{ij,g}$ are the lower and upper confidence intervals from the bootstrap estimation.

A positive NSSD value indicates stronger contribution of the j th HC salience to the i th cortical LV compared to the j th TRS salience. Similarly, a negative NSSD value indicates that the j th TRS salience contributes more strongly to the i th cortical LV compared to the j th HC salience. Saliences contributing equally to the i th cortical LV across both groups will have lower NSSD values.

3.4. Supplementary Post-hoc analyses

Cortical volumes are a product of cortical thickness and surface area. Given the different genetic and environmental influences on these two measures (Panizzon et al., 2009; Rakic et al., 1988; Habets et al., 2011), in supplementary analyses we applied our MB-PLS-C framework separately across cortical thickness and surface area in order to determine whether our volumetric findings were driven by thickness, surface area, or both. To assess the similarity between naturally occurring variations in cortical volumes and the latent cortical patterns from the MB-PLS-C analysis, correlations between the allometric scaling maps (Reardon et al., 2018) and latent cortical patterns were computed. Further details

are provided in the *Supplementary Materials*.

In the TRS group, the associations between significant LVs and confounding variables (chlorpromazine equivalent dose, tobacco, cannabis, alcohol use and PANSS positive, negative and general scores.) were assessed post hoc using Spearman's rank correlation analysis. Details are provided in *Supplementary Materials*.

4. Results

4.1. Univariate assessments

Patients with TRS and HCs showed no significant differences in age, sex and total intracranial volume (Table 2).

4.2. Two-group PLS

4.2.1. Latent components of multiblock cross-correlation matrix, R

The two-group MB-PLS-C analyses were significant (omnibus test, p = 1e-4). The singular value decomposition of *the input multiblock correlation matrix,* ***R****,* into additive components, described component-specific correlations between cortical volumes and cognitive variables and covariates in the latent space (Fig. 1). Two significant LVs were present, explaining 92.33% of sum-of-squares block covariance (Table 3). Below, we separately present the two latent patterns pertaining to these two LVs.

Table 2
Demographic and clinical characteristics of participants with treatment resistant schizophrenia and healthy controls.

Characteristic	Participants with treatment resistant schizophrenia (n = 41)		Healthy controls (n = 45)		Test statistic
	n	%	n	%	
Male	29	70.73	30	66.67	$\chi2 = 0.76$
	Mean	**SD**	**Mean**	**SD**	
Age	38.56	9.12	40.26	10.68	$U = 846$
BMI, kg/cm^2	30.90	6.96	24.24	5.93	$t = 4.78$*
Chlorpromazine equivalent dose	881.54	563.76	–	–	–
Modified PANSS†					
Positive	15.77	6.11	7.29	0.66	$\chi2 = 55.18$*
Negative	15.26	6.06	6.75	1.18	$\chi2 = 49.59$*
General	27.82	7.08	15.71	1.16	$\chi2 = 62.48$*
Total	58.84	16.17	29.77	2.21	$\chi2 = 58.69$*
GAF	49.62	14.44	80	11.71	$\chi2 = 42.26$*
SOFAS	49.84	14.82	80.31	11.88	$\chi2 = 44.28$*
Illness duration – psychotic symptoms, years	16.85	7.51	–	–	–
Intracranial Volume, mm^3	1.57e6	1.60e5	1.53e6	1.49e5	‡$F = 0.42$
Total brain volume (without ventricles), mm^3	1.13e6	1.21e5	1.15e6	1.19e5	‡$F = 3.26$ ‡‡$F = 21.06$*

* $p < 0.01$.

† Metrics n4 (Lack of spontaneity and flow of conversation) and g16 (Active social avoidance) were excluded from calculations due to incomplete data, Total score min = 28, max = 196.

‡ The *F*-statistic reports the group effect in the analysis of covariance with sex and age as covariates.

‡‡ This *F*-statistic reports the group effect in the analysis of covariance with total intracranial volume, sex and age as covariates.

4.2.2. First latent pattern

The first latent component, LV1 (identified in Fig. 1B and Table 3), explained 78.86% of the variance (p = 1e-4), and identified overall negative associations between brain regional volumes and cognitive measures in both patients and controls. The covariate blocks for LV1 revealed that total intracranial volume and male sex were positively associated with cortical volumes, whereas BMI was negatively correlated across both groups.

The cortical volume saliences in LV1 described a common cortical pattern shared by both TRS patients and HC groups, as all reliable saliences were negatively weighted (Fig. 2A-B). In TRS individuals, largest saliences were present in the frontal, temporal and parietal regions: lef superior temporal and supramarginal gyri and right inferior temporal, precentral, and middle temporal regions. In contrast, the largest contributions to the pattern in HC were observed in frontal, cingulate and occipital regions: right medial orbitofrontal cortex, isthmus of cingulate gyrus, lateral occipital regions and left rostral middle frontal gyrus.

The shared cognitive pattern in LV1 contained reliable contributions from IED-ES, PAL-TE, SSP-SL, SWM-S, and SMW-TE variables (See Table 1 for task descriptions). The pattern mapped more strongly to the TRS group (Fig. 2C). The LV-specific NSSD metric described the degree of group differences in the cortical saliences (Fig. 2D and Table S4). In LV1, the strongest NSSD regions in the HC group were the cuneus, pericalcarine and the isthmus region of the cingulate gyrus bilaterally. Strongest NSSD regions in the TRS group were the precentral gyrus bilaterally, right entorhinal and left posterior cingulate, medial orbitofrontal and superior temporal regions.

Within the training sample, cortical LV1 correlated strongly with cognition LV1 in the TRS group ($r = 0.53$, $p = 0.002$) and moderately in the HC group ($r = 0.37$, $p = 0.044$) (Fig. 2E). Similar correlations were observed in out-of-sample and cross-validated data. In LV1, significant moderate cortico-cognition correlations remained after covariate adjustment in the TRS group ($r = 0.46$, $p = 0.002$) and the HC group ($r = 0.30$, $p = 0.037$) (Fig. 2F). The difference in correlations between the two groups was not significant (z = -0.88, $p = 0.19$). For the cortical and cognitive saliences, a converging trend was found after 20 samples per group suggesting high stability of LV1 in both TRS and HC groups (Fig. 2G-H).

4.2.3. Second latent pattern

In contrast to LV1, the second latent component, LV2 (explained 13.47% of the variance, p = 8e-4), identified in Fig. 1C and Table 3, showed group-wise differences between cognition-cortical volume correlations. In TRS, overall negative correlations were present between cortical volumes and cognitive variables. Conversely, in HC, the cognitive measures generally correlated positively with the cortical volumes.

In the TRS group, the strongest reliable saliences were present in cingulate and temporal regions: the caudal anterior cingulate cortex and the superior temporal, inferior temporal and rostral middle frontal gyri in the left hemisphere and the inferior and middle temporal gyri in the right hemisphere (Fig. 3A-B). In the HC group, largest saliences were observed in frontal and temporal regions: inferior temporal, superior frontal and medial orbitofrontal gyri in the left hemisphere and the superior frontal and paracentral gyri in the right hemisphere.

The differential cognitive-structural pattern (in cingulate and temporal regions) between TRS and HC constituted reliable contributions from IED and PAL (Fig. 3C). In LV2, stronger NSSD regions in the HC group were the bilateral superior frontal, left precuneus and rostral anterior cingulate, right pars triangularis, paracentral and superior temporal regions. Moderately stronger NSSD regions in the TRS group were observed in left parahippocampus, right entorhinal, lingual, supramarginal and inferior temporal regions, indicating larger weights of these regions in the TRS cortical LV2 compared to controls (Fig. 3D and Table S4).

In the training sample, cortical LV2 correlated moderately to cognition LV2 in the TRS group ($r = 0.57$, $p = 8.8e-4$) and weakly in the

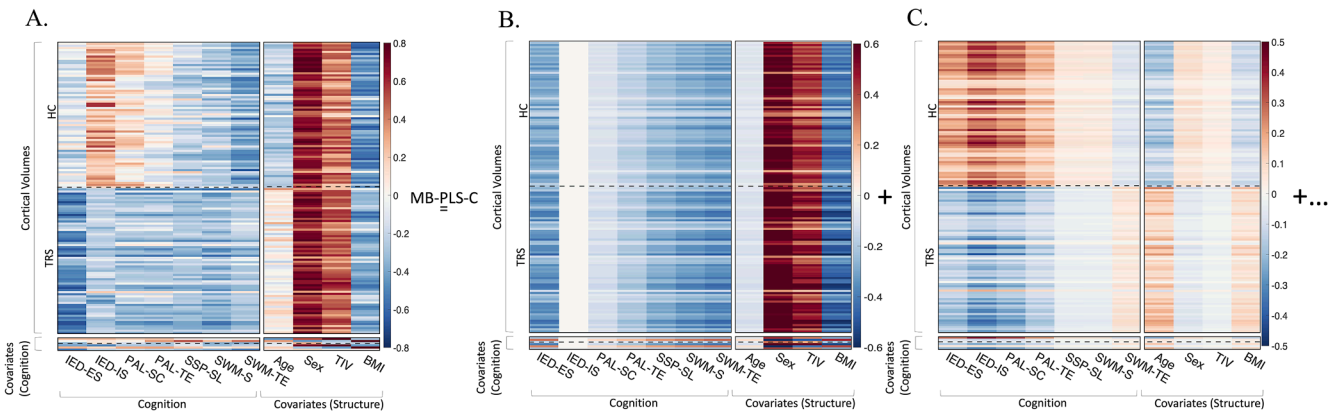

Fig. 1. Decomposition of input multiblock cross-correlation matrix into additive components using MB-PLS-C framework. A) The input matrix is composed of four disjoint data blocks with multivariate measures of brain structure, cognition and covariates (30 HC, 30 TRS). B-C) The first two components corresponding to the significant latent variables, LV1 and LV2, describe correlations in the latent space between cortical, cognitive and covariate measures across patients and healthy controls (right side of the equation).

Table 3
Block-wise contributions of latent variables to the singular values of the significant latent components (LV1 and LV2) and sum-of-squares covariance explained.

Latent component	Contribution to σ_i* (%)				Sum-of-squares covariance, ξ_i* (%)	*p*-value
	block 1 ($L_X^T L_Y$)	block 2 ($L_X^T L_{C_X}$)	block 3 ($L_{C_Y}^T L_Y$)	block 4 ($L_{C_Y}^T L_{C_X}$)		
LV1	31.62	1.04	64.98	2.36	78.86	1e-4
LV2	80.66	3.08	15.7	0.54	13.47	8e-4

* σ_i and ξ_i are the singular value and percent sum-of-squares crossblock covariance corresponding to the *i*th significant LV, $i \in \{1,2\}$. See East. S3, S4 and S5.

HC group ($r = 0.28$, $p = 0.13$) (Fig. 3E). The cross-validated and out-of-sample data showed generalizable correlations in the TRS group, and unreliable correlations in the HC group, demonstrating reliable cortico-cognitive coupling only in the individuals with TRS. An important point to note here is the inversion of the polarity of the correlations between cortical LV2 and cognition LV2 in the TRS group, as the negative saliences in the product defined by Eq. S2 (*Supplementary Material*) flip the direction of associations in the latent space, therefore, care must be taken in the interpretation of the latent patterns in a clinical context.

After covariate adjustment, moderate positive correlations were observed between cortical and cognition dimensions ($r = 0.36$, $p = 0.028$) in the TRS group and no significant correlations were observed in the HC group (Fig. 3F). Significant differences between the correlation coefficients of TRS and HC groups were present ($z = -2.07$, $p = 0.02$), suggesting significant cortico-cognition associations in the TRS group only (Fig. 3G). The cortical and cognitive saliences showed a converging trend after 20 participants per group (Fig. 3G-H).

4.3. Three-group PLS

4.3.1. Three-group input multiblock cross-correlation matrix

The three-group input cross-correlation matrix described correlations between data blocks and covariate blocks (Figure S10) in the HC, TRS and NAR groups. In the NAR group, mostly negative correlations were observed between cortical volumes and IED, SSP and SWM measures. Positive cortico-cognitive correlations were present mostly between PAL and cortical volumes. Cognitive variables showed mixed correlations with cognitive covariates.

4.3.2. Latent components of three-group multiblock cross-correlation matrix

The three-group MB-PLS-C analyses were significant (omnibus test, $p < 1e\text{-}6$). The singular value decomposition of $\boldsymbol{R}$, into additive components described component-specific latent cortico-cognitive associations (Figure S11). Two significant LVs explained 84.39% of block covariance.

The first latent variable, LV1 (explained sum-of-squares variance 71.19%, $p < 1e\text{-}6$), identified negative cortico-cognitive associations in the HC, TRS and NAR groups, except for cortico-PAL-SC associations where mostly positive correlations were observed. TIV and sex showed strong positive correlations with cortical volumes, whereas BMI was negatively correlated across all three groups.

The second latent variable, LV2 (explained sum-of-squares variance 12.47%, $p = 0.021$), showed group-wise differences between cognitive variables and cortical volume correlations. In the TRS group, overall negative correlations were present between cortical volumes and cognitive variables, except in SWM-TE which showed weak positive correlations with the cortical volume measures. In HC, the trends were reversed with cognitive measures correlating positively with cortical volumes, except in the case of SWM-TE. NAR showed weak cortico-cognitive correlations and the overall pattern matched more closely to the HC group.

4.3.3. Three-group patterns of cortical and cognitive saliences

For LV1, the cortical volume saliences described a common cortical pattern shared by all three groups with negatively weighted reliable saliences (Fig. 4A-B). In individuals with TRS, largest saliences were present in the temporal, parietal, cingulate and frontal regions. In the HC group, the largest contributions to the pattern came from the frontal and temporal regions. Strongest contributions in NARs were present in parietal and occipital structures. The cognitive pattern contained reliable contributions from IED-ES, SSP-SL, SWM-S and SMW-TE variables (Fig. 4C). No definite trend was observed between the sample size and LV1 saliences (Fig. 4D-E).

LV2 described a differential pattern of cortical regions, with positive reliable saliences in the HC and NAR groups, and negative reliable saliences in the TRS group (Fig. 5A-B). In the TRS and HC groups, strongest reliable saliences were present in the cingulate, frontal, and temporal regions. Occipital, frontal, cingulate and temporal regions were the strongest contributor to the NAR pattern. The cognitive pattern had reliable contributions from IED and PAL measures and the TRS group mapped in the opposite direction to the HC and NAR groups (Fig. 5C). The cortical and cognitive saliences showed a converging trend after 15 participants per group (Fig. 5D-E).

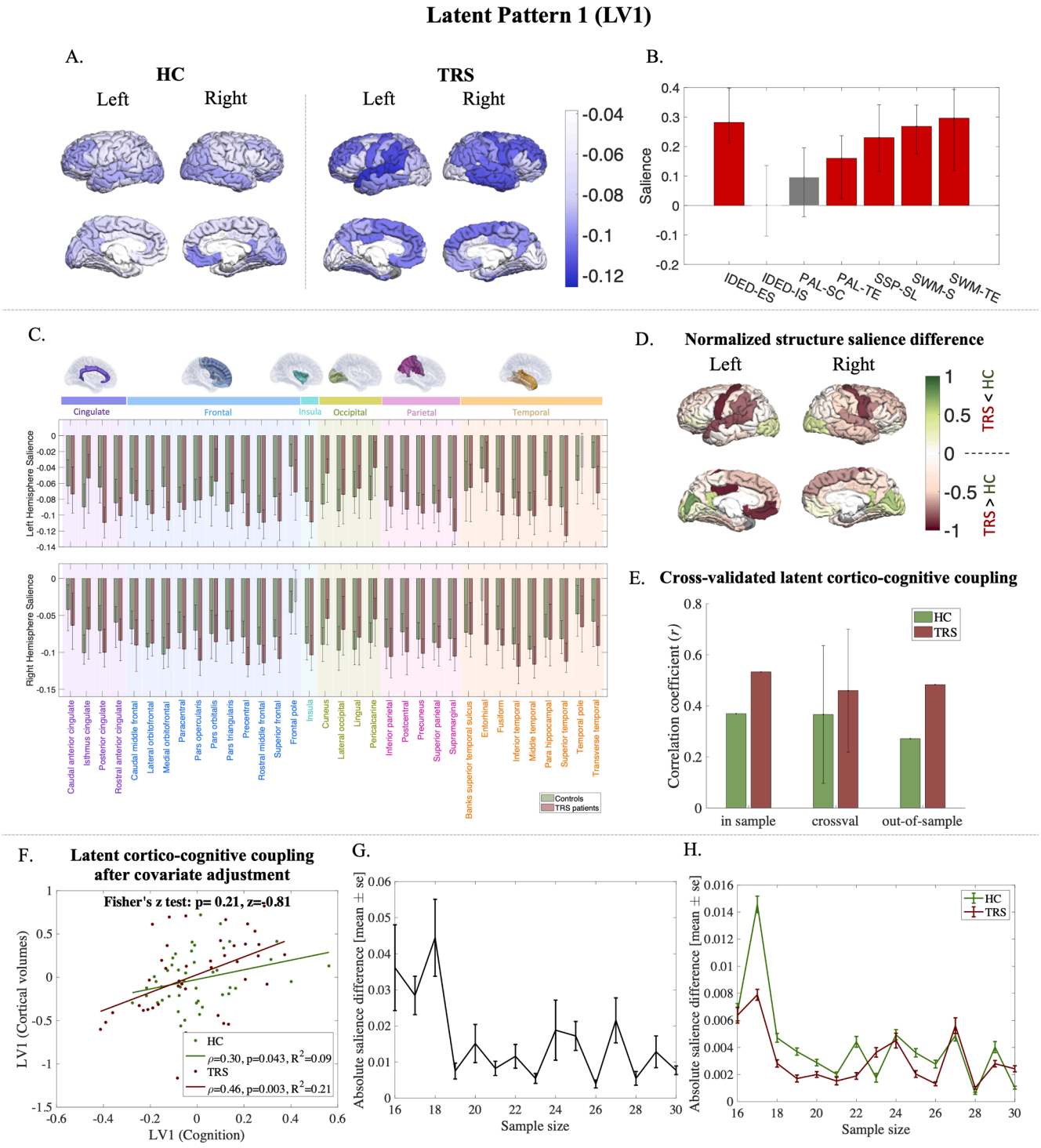

Fig. 2. The first latent cortico-cognitive pattern. A) Group-specific cortical saliences (weights of cortical variables) in the healthy controls (HC) and TRS patients. B) Common between-group cognitive saliences. Reliable contributions from all cognitive variables, except IED-IS and PAL-SC. C) A bar graph of group-wise cortical saliences in the HC (green) and TRS (red) groups with 95% confidence intervals (black lines) and color-coded lobe information. All reliable cortical saliences are negative. D) Regional Normalized structure salience difference between the HC and TRS groups. A positive value (green) indicates stronger regional salience in the HCs and a negative value (red) shows stronger TRS saliences. E) LV1 Cortico-cognitive correlations in the training and test samples, and the mean, and standard deviation of the distribution of correlation coefficients from Monte Carlo cross-validation. F) Post hoc latent cortico-cognitive correlations after LV-specific covariate adjustments. Significant moderate correlations in both groups. Non-significant Fisher's r-to-z test suggests no between-group differences in LV1 cortico-cognitive coupling. G-H) The effect of sample-size on salience strength. The cortico-cognitive patterns converge after 20 samples per group.

4.3.4. *Three-group covariate adjustment in latent space*

For each significant LV, the effects of covariate LVs were regressed out from corresponding cortical and cognitive LVs (Figure S14). In LV1, no significant cortico-cognition correlations were observed after covariate adjustment. For LV2, strong positive cortico-cognitive correlations were observed ($\rho = 0.53$, $p = 0.010$) in the NAR group and no significant correlations were observed in the HC and TRS groups. A significant difference between the correlation coefficients of TRS and HC

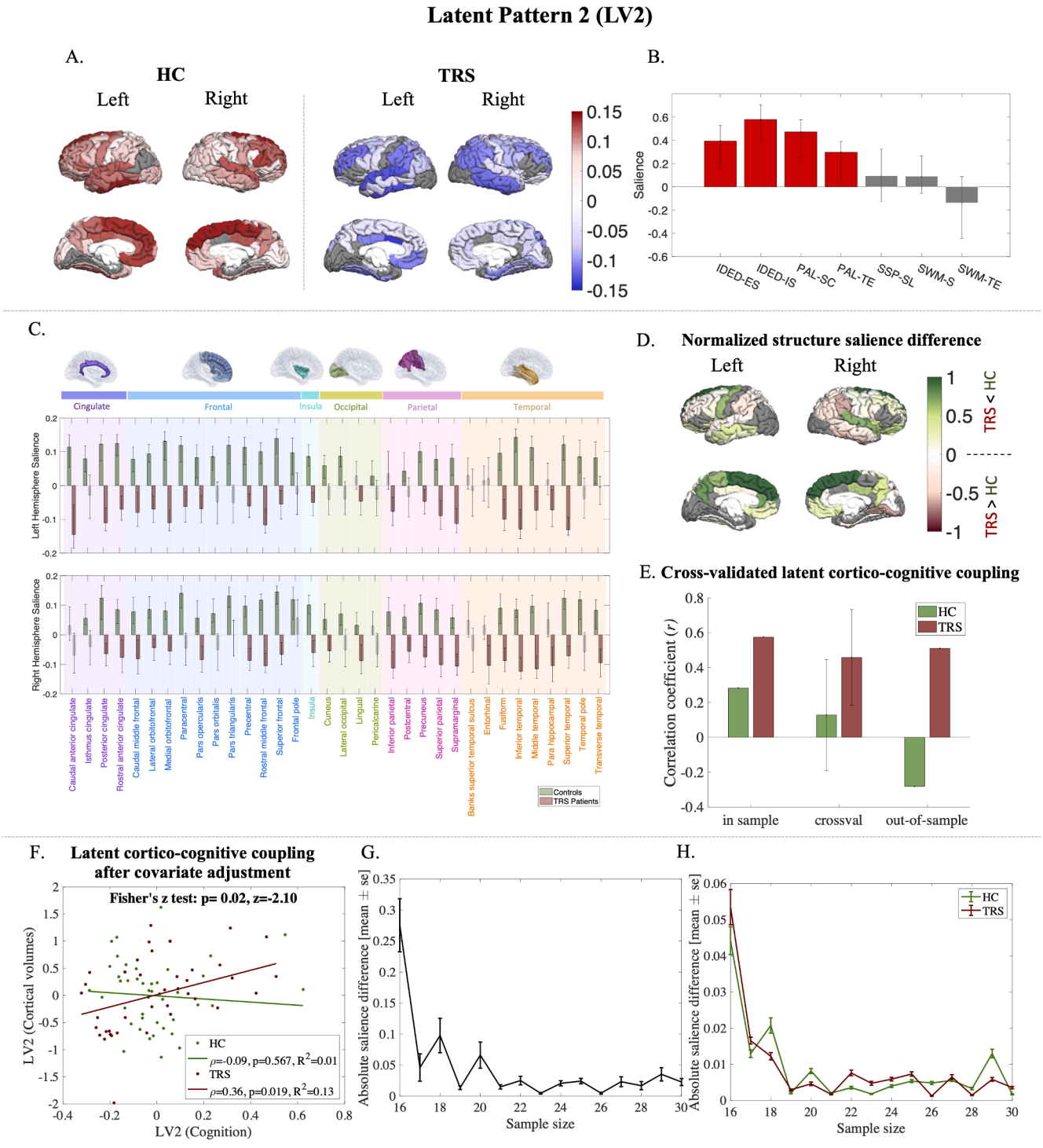

Fig. 3. The second latent cortico-cognitive pattern. A) Group-specific cortical saliences (weights of cortical variables) in the healthy controls (HC) and TRS patients showing a differential cortical pattern between groups. B) Common between-group cognitive saliences. Only PAL and IED related variables contributed significantly to the pattern. C) A bar graph of group-wise cortical saliences in the HC (green) and TRS (red) groups with 95% confidence intervals (black lines) and color-coded lobe information. All reliable cortical saliences are negative in TRS patients and positive in HCs. D) Regional Normalized structure salience difference between the HC and TRS groups. A positive value (green) indicates stronger regional salience in the HCs and a negative value (red) shows stronger TRS saliences. E) LV2 cortico-cognitive coupling in the training and test samples, and the mean, and standard deviation of the distribution of correlation coefficients from Monte Carlo cross-validation. Generalizable cortico-cognitive correlations only in the TRS group. F) Post hoc latent cortico-cognitive correlations after LV-specific covariate adjustments. Significant moderate correlations in the TRS group. Significant Fisher's r-t-z test suggests reliable cortico-cognitive coupling only in the TRS group. G-H) The effect of sample-size on salience strength. The cortico-cognitive patterns converged after 20 samples per group.

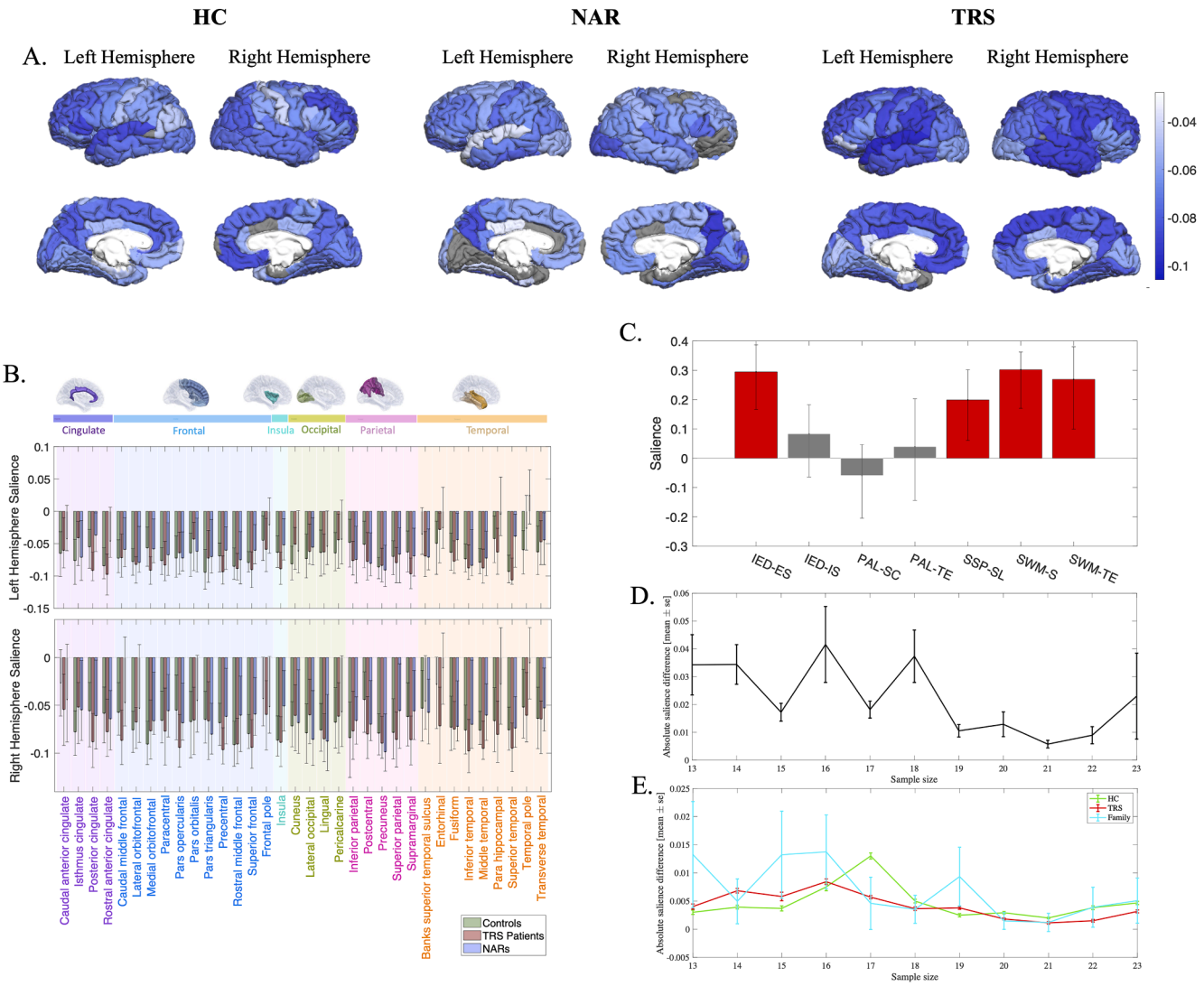

Fig. 4. The first latent cortico-cognitive pattern from three-group MB-PLS-C. A) Group-specific cortical saliences (weights of cortical variables) in the HC, TRS and NAR groups. B) A radial bar graph of group-wise cortical saliences with 95% confidence intervals (black lines) and color-coded lobe information. All reliable cortical saliences are negative. C) Cognitive saliences from averaged cognitive performance across both groups. IED-IS and PAL measures contributed unreliably to the pattern, whereas similar contributions to the cognitive pattern arose from IED-ES and SWM measures. D) The effect of sample-size on salience strength.

groups was present ($z = -2.07$, $p = 0.02$,), suggesting a significant cortico-cognition association in the TRS group only. Fisher's z-test between HC-TRS, HC-NAR and TRS-NAR showed no significant correlation differences between groups in both LV1 and LV2.

4.3.5. *Supplementary posthoc analyses*

Two-group MB-PLS-C using cognitive measures and cortical surface area revealed two significant LVs, explaining 92.32% of sum-of-squares block covariance. These latent variables closely resembled those observed in our cortical volume analyses, with LV1 identifying overall negative associations between brain cortical surface area and cognitive measures in both patients and controls (Figure S5), and LV2 identifying group-wise differences between cognition-cortical surface area correlations (Figure S6). The cognitive tasks and brain regions contributing to these LVs overlapped substantially with those observed in the two-group MB-PLS-C using cortical volumes.

Conversely, two-group MB-PLS-C using cognitive measures and cortical thickness revealed only one significant LV, explaining 60.82% of the variance. This LV identified a common cortical pattern shared by both TRS patients and HC groups (Figure S7).

The comparison between the allometric scaling maps from (Reardon et al., 2018) and the latent cortical volume patterns from LV1 and LV2 showed that the allometric scaling maps were significantly correlated to cortical patterns in LV1 bilaterally across both TRS and HC groups. However, in LV2, significant correlations between the allometric scaling were only observed in the healthy controls. Further details are provided in the *Supplementary Materials*.

Significant correlations were found between PANSS negative scores and cortical and cognitive LVs 1 and 2. PANSS general scores also significantly correlated with cortical and cognitive LVs 1 and 2. No significant correlations were found between latent variables and clozapine equivalent dose, tobacco, cannabis, alcohol use and PANSS positive scores. Details provided in *Supplementary Materials*.

5. Discussion

This is the first study to use a novel multivariate pattern analysis (MB-PLS-C) of brain gray matter structure and cognition in treatment-resistant schizophrenia (TRS) patients compared with healthy controls (HC) and non-affected relatives (NAR) of TRS patients. As expected, univariate analyses showed gross impairments in TRS in both brain structural and cognitive domains. In the two-group MB-PLS-C analysis

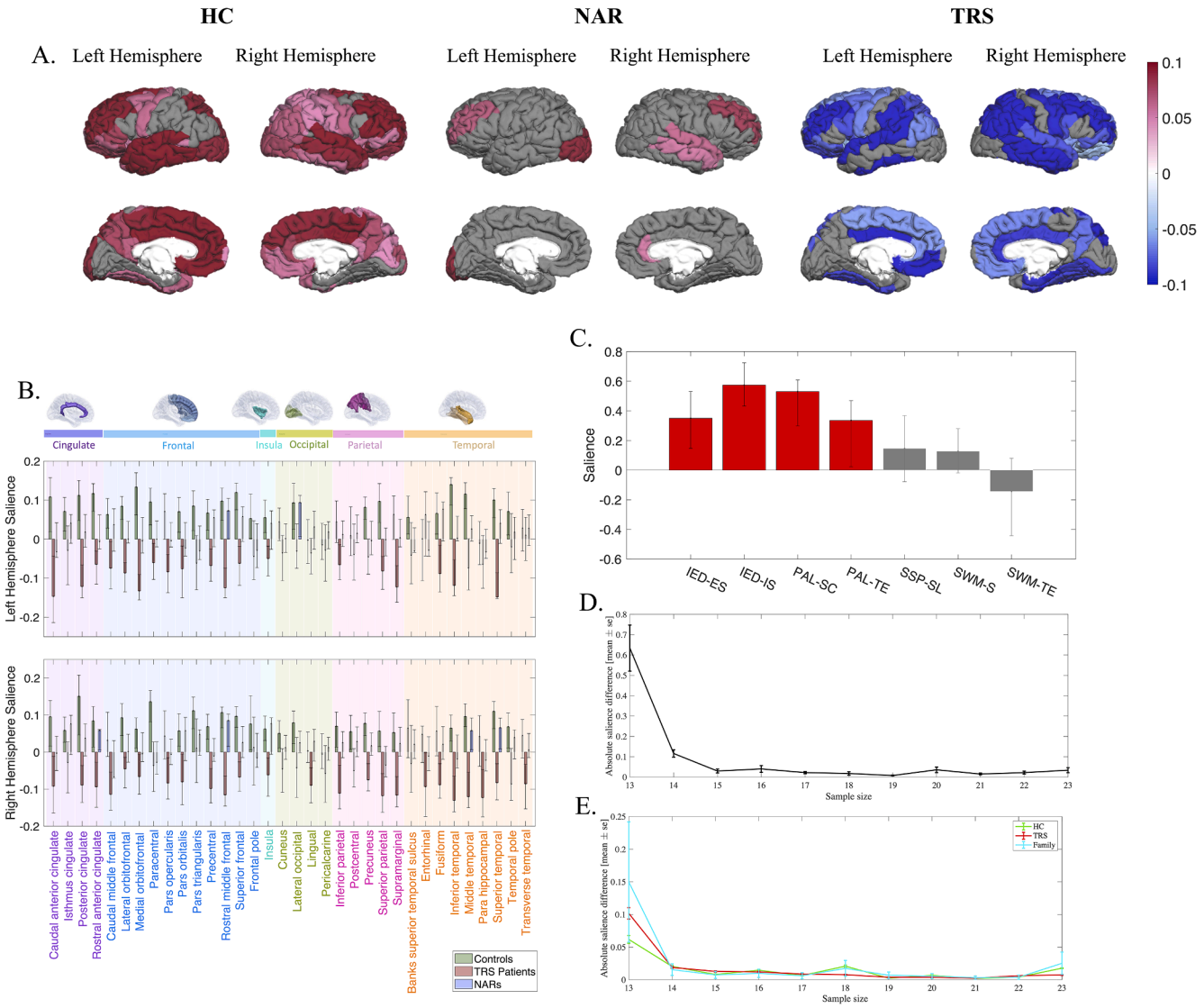

Fig. 5. The second three-group latent cortico-cognitive pattern. A) Group-specific cortical saliences (weights of cortical variables). B) A bar graph of group-wise cortical saliences with 95% confidence intervals (black lines) and color-coded lobe information. All reliable cortical saliences are negative in the TRS group and positive in the HC and NAR groups. C) Cognitive saliences from averaged cognitive performance across both groups. Only IED and PAL measures contributed reliably to the pattern. D) The effect of sample-size on salience strength. The cortical and cognitive patterns start converging after 15 samples per group.

(TRS and HC), we identified a two-component latent signature of TRS which collectively explained > 90% of the sum-of-squares variance (LV1 and LV2). The first component described a pattern of cortico-cognitive coupling shared by both HCs and TRS patients. The second component indexed a differential pattern, with only TRS patients demonstrating a reliable pattern, suggesting a possible TRS-specific signature. In supplementary three-group analyses incorporating NARs, a similar two-component latent signature was observed (>90% of sum-of-squares variance explained), with a shared first component across the three groups and a differential second component. The NAR group better matched the HCs in both components.

In the main TRS *vs* HC analysis, LV1 explained ~ 79% of the sum-of-squares variance and was significant in both groups. TRS patients showed a stronger mapping of brain structural profile to the pattern of cognitive deficits than did HCs, however, in post hoc analyses there was no statistically significant between-group differences in the LV1 cortico-cognitive coupling. Statistically reliable cognitive measures in LV1 arose predominantly from measures of executive function (spatial working memory, spatial short-term memory span, and attentional set-shifting) with a contribution from associative memory. LV1 was characterized by a global pattern of brain structure saliences, with relationships observed across widespread cortical regions in both TRS patients and HCs. In both groups, larger volumes were associated with better cognitive performance across multiple tasks, suggesting that LV1 may capture neurodevelopmentally-driven global cognitive capacity that is relevant to both TRS patients and healthy people. Indeed, our previously reported PLS-C analyses in an independent cohort of antipsychotic-naive, first-episode schizophrenia patients also revealed that spatial working memory mapped to a global, shared brain structural pattern in both patients and controls and, similar to the current study, the pattern was stronger in patients (Jessen et al., 2019). Taken together, these studies indicate the pattern represented by LV1 would be consistent with a neurodevelopmentally derived pattern that is not unique to schizophrenia. Further evidence to support the neurodevelopmental underpinnings of LV1 comes from our supplementary analyses, which demonstrated that this LV is driven primarily by surface area, which is largely determined during prenatal development, rather than cortical thickness, which changes dynamically across the lifespan (Panizzon et al., 2009; Rakic et al., 1988; Habets et al., 2011). Furthermore, TRS patients and healthy controls demonstrated significant correlations

between their LV1 cortical patterns and the allometric scaling maps reported by (Reardon et al., 2018), which capture naturally occurring variations in total cortical area that are evolutionary- and developmentally-driven.

In contrast, the *differential* pattern of brain structure-cognition relationships identified in LV2, (explaining ~ 13.5% of the sum-of-squares variance), suggested a specific signature distinguishing TRS patients from healthy individuals. Statistically reliable cognitive measures in LV2 included associative memory and attentional set-shifting ability. Interestingly, both the brain regions and cognitive tasks implicated in LV2 have been shown evidence of decline across illness stages, (Pantelis et al., 2009; Leeson et al., 2009) indicating that LV2 may represent illness-specific neuroprogressive processes in TRS patients. In an independent sample, we previously demonstrated that performance on the PAL task deteriorates over time in individuals with schizophrenia-spectrum disorders following psychosis onset (Wannan et al., 2018). Similarly, IED performance has been shown to be more strongly impaired in individuals with chronic schizophrenia compared to those with first-episode psychosis, suggestive of deterioration of this ability over the course of the illness (Pantelis et al., 2003; Pantelis et al., 2009; Hutton et al., 1998; Pantelis et al., 1999). Accordingly, we did not observe a relationship between IED and brain structure in our PLS-C analyses of antipsychotic-naive, first-episode schizophrenia patients (Jessen et al., 2019). Furthermore, the strongest brain structure saliences associated within LV2 in patients were observed across the frontal and temporal lobes, regions which demonstrate progressive grey matter loss across numerous longitudinal studies (Dietsche et al., 2017; Pantelis et al., 2003), including at transition to psychosis. These frontal and temporal regions, (Fernandes et al., 2004; Jemel et al., 2003; Aalto et al., 2005; Henson and Fletcher, 2001) along with the posterior parietal lobe, which was also implicated in the patient group, are heavily implicated in performance on both memory and attentional tasks (Ciaramelli et al., 2008; Ciaramelli et al., 2020; Uncapher and Wagner, 2009; Berryhill and Olson, 2008). Thus, our findings suggest there may be a dynamic interplay between gray matter volume in these regions, which consistently show longitudinal volume reductions in schizophrenia, and performance on the PAL and IED tasks in those who develop TRS. Furthermore, the lack of associations between the LV2 cortical pattern in the TRS group and the allometric scaling maps point towards the illness-specific origins of the LV2 cortical pattern which is different from the naturally occurring variations in the cortical volumes. Interestingly, the LV2 cortical pattern in the healthy controls correlated strongly with the allometric scaling maps, further evidencing that the differential LV2 cortical pattern is arising from illness-specific mechanisms.

In the MB-PLS-C analyses, the novel latent variable-specific representation of the covariate blocks enables assessment of the confounding effects in the latent space instead of through pre-PLS-C data residualization, and hence offers the ability to control for the LV-specific confounding effects. (Syeda et al., 2021) The proposed normalized structure salience difference (NSSD) identifies regions of most reliable structure salience differences between groups. The group differences in the latent variables can arise from two factors: 1) Differences in the original data, i.e., group differences in the raw data are preserved in the latent space, and/or 2) group-differences in the cortical pattern (region- and group-wise saliences). The NSSD identifies the regions with largest group-differences in the cortical pattern whilst suppressing the regions contributing equally to the pattern across both groups, thereby isolating the foci of differences in cortical signatures for TRS compared with HC.

In LV1, the NSSD metrics of healthy controls showed a stronger differential mapping of brain regions associated with visual information processing (cuneus, pericalcarine regions) onto the common cognitive pattern. Conversely, TRS patients showed a stronger mapping of fronto-temporal association areas onto the common cognitive pattern. In LV2 HCs had the largest NSSD metrics in higher-order association areas in frontal, temporal, and parietal cortices. Interestingly, in post-hoc analyses, the cortico-cognitive coupling was absent in healthy controls, suggesting that volume losses in healthy controls in these regions do not correlate to the LV2 pattern of cognitive deficits, and therefore may not represent pathological processes. Thus, healthy individuals may have a higher degree of cortico-cognitive flexibility and greater latitude in brain structure, such that minor changes are not associated with impaired performance, indicative of greater cognitive reserve in healthy persons. In TRS patients, temporal and parietal lobe volume reductions were strongly coupled with impairments in associative memory and attentional set-shifting. Post-hoc analyses also revealed significant latent cortico-cognitive coupling in TRS patients. The presence of significant brain structure-cognition relationships in TRS patients but not healthy controls may represent loss of brain plasticity and compensatory processes in TRS patients, reflecting disease-related pathology. Interestingly, in our previous PLS-C analyses of antipsychotic-naive patients, brain structure was largely preserved, compared to HCs, yet the cortico-cognitive coupling was also only present in patients. Thus, even in the absence of apparent brain volume loss, patients at the earliest stage of schizophrenia are dependent on brain structure when cognitively challenged (Jessen et al., 2019).

Potential confounding factors of current antipsychotic medication dosage and substance use did not explain brain or cognitive saliences in either LVs (*Supplementary Material*). This is particularly relevant for LV2, which appears to represent a *'TRS signature'*, and suggests that these cortico-cognition relationships are not driven by antipsychotic medication or substance use. Significant relationships were observed between brain structure and cognition saliences and PANSS negative and general symptoms in both LVs. These findings are consistent with previous studies, which have found that cognitive and negative symptoms are not only correlated in their severity in schizophrenia, but also share similar onset, temporal course, prognostic importance, and correlations with functional outcomes (Harvey et al., 2006). Our findings are also consistent with previous PLS studies, which found stronger loading for negative symptoms rather than positive symptoms in relation to brain structure (Kirschner et al., 2020).

In our supplementary analyses, we conducted a 3-group PLS analysis including a smaller sample of non-affected first-degree relatives of the TRS patients. Consistent with our two-group analysis, this 3-group PLS identified two LVs. $LV1_{3\text{-group}}$ captured a common pattern of brain structure-cognition relationships across all three groups, with strong similarity to the two-group cognitive pattern in LV1. In unaffected family members, the strongest $LV1_{3\text{-group}}$ saliences were observed in the precuneus bilaterally. This brain region is known to be implicated in response inhibition, shifting attention between motor targets, and visuospatial mental operations, which would be key functions that are required for successful performance on the touchscreen CANTAB tasks. $LV2_{3\text{-group}}$ also showed a similar pattern of brain structure-cognition relationships as seen in our two-group analysis, with the PAL and IED tasks once again contributing to this LV.

Our findings should be considered in the context of several limitations. A major limitation of the study is the absence of a treatment-responsive or medication-naïve schizophrenia sample with which to compare our TRS sample. Thus, it is not possible to determine whether the observed pattern is unique to TRS, or whether it represents a broader signature for schizophrenia or antipsychotic usage. Future studies including a treatment-responsive sample are needed to address this limitation. In addition, PLS analyses are complex multivariate models and in the current analyses the number of input variables exceeds the number of subjects. To minimize the risk of overfitting, we established the statistical validity of the patterns by running a number of non-parametric tests (data provided in Figs. 2 and 3, panels D and E). In the two-group analyses, the cortical and cognitive saliences converged after 20 participants per group (Fig. 2G-H, 3G-H), suggesting sufficient power in our main analyses. Although our novel MB-PLS-C framework enabled modelling of the effects of age, sex, total intracranial volume, and BMI which are shared between groups, the potential confounding

effect of illness-related factors such as life-time medication exposure and substance use could not be integrated in the PLS model. Our finding that medication exposure and substance use did not explain our findings are therefore based on post-hoc correlational analyses between the variables and the identified LVs. Finally, data were not available to determine response to clozapine, and therefore we were unable to identify individuals who were potentially ultra-treatment-resistant.

In summary, our novel extended multiblock PLS-C approach suggests a widely shared pattern of cortico-cognitive relationships in TRS patients and HC (LV1). However, ~13% of the cortico-cognitive relationships revealed a differential pattern of relationships between TRS and HC (LV2). The opposing pattern of brain structure-cognition relationships seen in LV2 was specifically driven by PAL and IED, with the strongest cortical saliences observed across the frontal and temporal lobes - regions which are more severely affected as the illness becomes more chronic. This dissociable pattern may provide a signature of TRS, though comparison with a treatment-responsive sample is needed to confirm whether this signature is TRS-specific. It is not known if such a signature is apparent from illness onset or evolves during its course, which should be investigated in future longitudinal studies of patients experiencing a first-episode of illness. Mapping the trajectory of TRS from illness onset would provide important information for early intervention to ameliorate or prevent TRS developing.

CRediT authorship contribution statement

Warda T. Syeda: Conceptualization, Methodology, Software, Validation, Formal analysis, Writing – original draft, Writing – review & editing, Visualization. **Cassandra M.J. Wannan:** Conceptualization, Methodology, Data curation, Writing – original draft, Writing – review & editing, Visualization, Investigation. **Antonia H. Merritt:** Data curation, Writing – review & editing, Project administration. **Jayachandra M. Raghava:** Software, Methodology, Writing – review & editing. **Mahesh Jayaram:** Writing – review & editing. **Dennis Velakoulis:** Writing – review & editing. **Tina D. Kristensen:** Writing – review & editing. **Rigas Filippos Soldatos:** Writing – review & editing. **Shane Tonissen:** Writing – review & editing. **Naveen Thomas:** Writing – review & editing. **Karen S. Ambrosen:** Writing – review & editing. **Mikkel E. Sørensen:** Writing – review & editing. **Birgitte Fagerlund:** Writing – review & editing. **Egill Rostrup:** Writing – review & editing. **Birte Y. Glenthøj:** Writing – review & editing. **Efstratios Skafidas:** Writing – review & editing. **Chad A. Bousman:** Writing – review & editing. **Leigh A. Johnston:** Conceptualization. **Ian Everall:** Writing – review & editing, Funding acquisition. **Bjørn H. Ebdrup:** Conceptualization, Methodology, Validation, Writing – original draft, Writing – review & editing, Visualization, Supervision. **Christos Pantelis:** Conceptualization, Methodology, Validation, Writing – original draft, Writing – review & editing, Visualization, Supervision, Resources.

Declaration of Competing of Interest

The authors declare no conflict of interest.

Acknowledgements

The authors thank Prof. Andrew Zalesky (Melbourne Neuropsychiatry Centre) for his insightful suggestions about the MB-PLS-C technique. CP received funding from National Health and Medical Research Council, Australia (1196508, 1150083). BE received funding from The Lundbeck Foundation, Denmark (R316-2019-191).

Appendix A. Supplementary data

Supplementary data to this article can be found online at https://doi.org/10.1016/j.nicl.2022.103064.

References

Aalto, S., Brück, A., Laine, M., Någren, K., Rinne, J.O., 2005. Frontal and temporal dopamine release during working memory and attention tasks in healthy humans: a positron emission tomography study using the high-affinity dopamine D2 receptor ligand [11C] FLB 457. J. Neurosci. 25 (10), 2471–2477.
Berryhill, M.E., Olson, I.R., 2008. Is the posterior parietal lobe involved in working memory retrieval?: Evidence from patients with bilateral parietal lobe damage. Neuropsychologia. 46 (7), 1775–1786.
Bowie, C.R., Harvey, P.D., 2006. Cognitive deficits and functional outcome in schizophrenia. Neuropsychiatr. Dis. Treat. 2 (4), 531–536.
Ciaramelli, E., Grady, C.L., Moscovitch, M., 2008. Top-down and bottom-up attention to memory: a hypothesis (AtoM) on the role of the posterior parietal cortex in memory retrieval. Neuropsychologia. 46 (7), 1828–1851.
Ciaramelli, E., Burianová, H., Vallesi, A., Cabeza, R., Moscovitch, M., 2020. Functional interplay between posterior parietal cortex and hippocampus during detection of memory targets and nontargets. Front. Neurosci. 14, 1164.
Desikan, R.S., Ségonne, F., Fischl, B., Quinn, B.T., Dickerson, B.C., Blacker, D., Buckner, R.L., Dale, A.M., Maguire, R.P., Hyman, B.T., Albert, M.S., Killiany, R.J., 2006. An automated labeling system for subdividing the human cerebral cortex on MRI scans into gyral based regions of interest. Neuroimage. 31 (3), 968–980.
Dietsche, B., Kircher, T., Falkenberg, I., 2017. Structural brain changes in schizophrenia at different stages of the illness: a selective review of longitudinal magnetic resonance imaging studies. Aust. N. Z. J. Psychiatry 51 (5), 500–508.
Fernandes, M.A., Davidson, P.S., Glisky, E.L., Moscovitch, M., 2004. Contribution of frontal and temporal lobe function to memory interference from divided attention at retrieval. Neuropsychology. 18 (3), 514.
Fischl, B., Van Der Kouwe, A., Destrieux, C., et al., 2004. Automatically parcellating the human cerebral cortex. Cereb. Cortex 14 (1), 11–22.
Goldman, H.H., Skodol, A.E., Lave, T.R., 1992. Revising axis V for DSM-IV: a review of measures of social functioning. Am. J. Psychiatry. 149, 9.
Habets, P., Marcelis, M., Gronenschild, E., Drukker, M., van Os, J., 2011. Reduced cortical thickness as an outcome of differential sensitivity to environmental risks in schizophrenia. Biol. Psychiatry 69 (5), 487–494.
Hall, R.C., 1995. Global assessment of functioning: a modified scale. Psychosomatics. 36 (3), 267–275.
Harvey, P.D., Koren, D., Reichenberg, A., Bowie, C.R., 2006. Negative symptoms and cognitive deficits: what is the nature of their relationship? Schizophr. Bull. 32 (2), 250–258.
Henson, R., Fletcher, P., 2001. Frontal lobes and human memory. Brain. 124, 849–881.
Hilker, R., Helenius, D., Fagerlund, B., Skytthe, A., Christensen, K., Werge, T.M., Nordentoft, M., Glenthøj, B., 2018. Heritability of schizophrenia and schizophrenia spectrum based on the nationwide Danish twin register. Biol. Psychiatry 83 (6), 492–498.
Holdnack, H., 2001. Wechsler test of adult reading: WTAR. The Psychological Corporation, San Antonio, TX.
Hutton, S., Puri, B., Duncan, L.-J., Robbins, T., Barnes, T., Joyce, E., 1998. Executive function in first-episode schizophrenia. Psychol. Med. 28 (2), 463–473.
Jemel, B., Oades, R.D., Oknina, L., Achenbach, C., Röpcke, B., 2003. Frontal and temporal lobe sources for a marker of controlled auditory attention: the negative difference (Nd) event-related potential. Brain Topogr. 15 (4), 249–262.
Jessen, K., Mandl, R.C., Fagerlund, B., et al., 2019. Patterns of cortical structures and cognition in antipsychotic-naïve patients with first-episode schizophrenia: a partial least squares correlation analysis. Biol. Psychiatry: Cognit. Neurosci. Neuroimaging. 4 (5), 444–453.
Kane, J., Honigfeld, G., Singer, J., Meltzer, H., 1988. Clozapine for the treatment-resistant schizophrenic: a double-blind comparison with chlorpromazine. Arch. Gen. Psychiatry 45 (9), 789–796.
Karantonis, J.A., Carruthers, S.P., Rossell, S.L., et al., 2021. A systematic review of cognition-brain morphology relationships on the schizophrenia-bipolar disorder spectrum. Schizophrenia Bull.
Kay, S.R., Fiszbein, A., Opler, L.A., 1987. The positive and negative syndrome scale (PANSS) for schizophrenia. Schizophr. Bull. 13 (2), 261–276.
Kirschner, M., Shafiei, G., Markello, R.D., et al., 2020. Latent clinical-anatomical dimensions of schizophrenia. Schizophrenia Bull. 46 (6), 1426–1438.
Kochunov, P., Fan, F., Ryan, M.C., et al., 2020. Translating ENIGMA schizophrenia findings using the regional vulnerability index: association with cognition, symptoms, and disease trajectory. Hum. Brain Mapp.
Krishnan, A., Williams, L.J., McIntosh, A.R., Abdi, H., 2011. Partial Least Squares (PLS) methods for neuroimaging: a tutorial and review. Neuroimage. 56 (2), 455–475.
Lecrubier, Y., Sheehan, D.V., Weiller, E., Amorim, P., Bonora, I., Sheehan, K.H., Janavs, J., Dunbar, G.C., 1997. The Mini International Neuropsychiatric Interview (MINI). A short diagnostic structured interview: reliability and validity according to the CIDI. European psychiatry. 12 (5), 224–231.
Leeson, V.C., Robbins, T.W., Matheson, E., Hutton, S.B., Ron, M.A., Barnes, T.R.E., Joyce, E.M., 2009. Discrimination learning, reversal, and set-shifting in first-episode schizophrenia: stability over six years and specific associations with medication type and disorganization syndrome. Biol. Psychiatry 66 (6), 586–593.
Mørup, M.F., Kymes, S.M., Oudin Åström, D., 2020. A modelling approach to estimate the prevalence of treatment-resistant schizophrenia in the United States. PloS one. 15 (6), e0234121.
Nucifora Jr, F.C., Woznica, E., Lee, B.J., Cascella, N., Sawa, A., 2019. Treatment resistant schizophrenia: clinical, biological, and therapeutic perspectives. Neurobiol. Dis. 131, 104257.

Panizzon, M.S., Fennema-Notestine, C., Eyler, L.T., et al., 2009. Distinct genetic influences on cortical surface area and cortical thickness. Cerebral Cortex. 19 (11), 2728–2735.
Pantelis, C., Barber, F.Z., Barnes, T.R., Nelson, H.E., Owen, A.M., Robbins, T.W., 1999. Comparison of set-shifting ability in patients with chronic schizophrenia and frontal lobe damage. Schizophr. Res. 37 (3), 251–270.
Pantelis, C., Velakoulis, D., McGorry, P.D., Wood, S.J., Suckling, J., Phillips, L.J., Yung, A.R., Bullmore, E.T., Brewer, W., Soulsby, B., Desmond, P., 2003. Neuroanatomical abnormalities before and after onset of psychosis: a cross-sectional and longitudinal MRI comparison. The Lancet 361 (9354), 281–288.
Pantelis, C., Wood, S.J., Proffitt, T.M., Testa, R., Mahony, K., Brewer, W.J., Buchanan, J.-A., Velakoulis, D., McGorry, P.D., 2009. Attentional set-shifting ability in first-episode and established schizophrenia: relationship to working memory. Schizophr. Res. 112 (1-3), 104–113.
Rakic, P., 1988. Specification of cerebral cortical areas. Science 241 (4862), 170–176.
Reardon, P.K., Seidlitz, J., Vandekar, S., Liu, S., Patel, R., Park, M.T.M., Alexander-Bloch, A., Clasen, L.S., Blumenthal, J.D., Lalonde, F.M., Giedd, J.N., Gur, R.C., Gur, R.E., Lerch, J.P., Chakravarty, M.M., Satterthwaite, T.D., Shinohara, R.T., Raznahan, A., 2018. Normative brain size variation and brain shape diversity in humans. Science 360 (6394), 1222–1227.
Spangaro, M., Martini, F., Bechi, M., Buonocore, M., Agostoni, G., Cocchi, F., Sapienza, J., Bosia, M., Cavallaro, R., 2021. Longitudinal course of cognition in schizophrenia: Does treatment resistance play a role? J. Psychiatr. Res. 141, 346–352.
Suzuki, T., Remington, G., Mulsant, B.H., Uchida, H., Rajji, T.K., Graff-Guerrero, A., Mimura, M., Mamo, D.C., 2012. Defining treatment-resistant schizophrenia and response to antipsychotics: a review and recommendation. Psychiatry Res. 197 (1-2), 1–6.
Syeda, W.T., Ebdurp, B.H., Wannan, C.M.J., et al., 2021. A multiblock partial least squares correlation framework for covariate adjustment and interpretation of multimodality neuroimaging data. ISMRM.
Uncapher, M.R., Wagner, A.D., 2009. Posterior parietal cortex and episodic encoding: insights from fMRI subsequent memory effects and dual-attention theory. Neurobiol. Learn. Mem. 91 (2), 139–154.
van Erp, T.G.M., Walton, E., Hibar, D.P., Schmaal, L., Jiang, W., Glahn, D.C., Pearlson, G. D., Yao, N., Fukunaga, M., Hashimoto, R., Okada, N., Yamamori, H., Bustillo, J.R., Clark, V.P., Agartz, I., Mueller, B.A., Cahn, W., de Zwarte, S.M.C., Hulshoff Pol, H.E., Kahn, R.S., Ophoff, R.A., van Haren, N.E.M., Andreassen, O.A., Dale, A.M., Doan, N. T., Gurholt, T.P., Hartberg, C.B., Haukvik, U.K., Jørgensen, K.N., Lagerberg, T.V., Melle, I., Westlye, L.T., Gruber, O., Kraemer, B., Richter, A., Zilles, D., Calhoun, V.D., Crespo-Facorro, B., Roiz-Santiañez, R., Tordesillas-Gutiérrez, D., Loughland, C., Carr, V.J., Catts, S., Cropley, V.L., Fullerton, J.M., Green, M.J., Henskens, F.A., Jablensky, A., Lenroot, R.K., Mowry, B.J., Michie, P.T., Pantelis, C., Quidé, Y., Schall, U., Scott, R.J., Cairns, M.J., Seal, M., Tooney, P.A., Rasser, P.E., Cooper, G., Shannon Weickert, C., Weickert, T.W., Morris, D.W., Hong, E., Kochunov, P., Beard, L.M., Gur, R.E., Gur, R.C., Satterthwaite, T.D., Wolf, D.H., Belger, A., Brown, G.G., Ford, J.M., Macciardi, F., Mathalon, D.H., O'Leary, D.S., Potkin, S.G., Preda, A., Voyvodic, J., Lim, K.O., McEwen, S., Yang, F., Tan, Y., Tan, S., Wang, Z., Fan, F., Chen, J., Xiang, H., Tang, S., Guo, H., Wan, P., Wei, D., Bockholt, H.J., Ehrlich, S., Wolthusen, R.P.F., King, M.D., Shoemaker, J.M., Sponheim, S.R., De Haan, L., Koenders, L., Machielsen, M.W., van Amelsvoort, T., Veltman, D.J., Assogna, F., Banaj, N., de Rossi, P., Iorio, M., Piras, F., Spalletta, G., McKenna, P.J., Pomarol-Clotet, E., Salvador, R., Corvin, A., Donohoe, G., Kelly, S., Whelan, C.D., Dickie, E.W., Rotenberg, D., Voineskos, A.N., Ciufolini, S., Radua, J., Dazzan, P., Murray, R., Reis Marques, T., Simmons, A., Borgwardt, S., Egloff, L., Harrisberger, F., Riecher-Rössler, A., Smieskova, R., Alpert, K.I., Wang, L., Jönsson, E.G., Koops, S., Sommer, I.E.C., Bertolino, A., Bonvino, A., Di Giorgio, A., Neilson, E., Mayer, A.R., Stephen, J.M., Kwon, J.S., Yun, J.-Y., Cannon, D.M., McDonald, C., Lebedeva, I., Tomyshev, A.S., Akhadov, T., Kaleda, V., Fatouros-Bergman, H., Flyckt, L., Busatto, G.F., Rosa, P.G.P., Serpa, M.H., Zanetti, M.V., Hoschl, C., Skoch, A., Spaniel, F., Tomecek, D., Hagenaars, S.P., McIntosh, A.M., Whalley, H.C., Lawrie, S. M., Knöchel, C., Oertel-Knöchel, V., Stäblein, M., Howells, F.M., Stein, D.J., Temmingh, H.S., Uhlmann, A., Lopez-Jaramillo, C., Dima, D., McMahon, A., Faskowitz, J.I., Gutman, B.A., Jahanshad, N., Thompson, P.M., Turner, J.A., Farde, L., Flyckt, L., Engberg, G., Erhardt, S., Fatouros-Bergman, H., Cervenka, S., Schwieler, L., Piehl, F., Agartz, I., Collste, K., Victorsson, P., Malmqvist, A., Hedberg, M., Orhan, F., 2018. Cortical brain abnormalities in 4474 individuals with schizophrenia and 5098 control subjects via the enhancing neuro imaging genetics through meta analysis (ENIGMA) consortium. Biol. Psychiatry 84 (9), 644–654.
Van Roon, P., Zakizadeh, J., Chartier, S., 2014. Partial least squares tutorial for analyzing neuroimaging data. Tutorials Quant. Methods Psychol. 10, 200–215.
Wannan, C.M.J., Bartholomeusz, C.F., Cropley, V.L., Van Rheenen, T.E., Panayiotou, A., Brewer, W.J., Proffitt, T.M., Henry, L., Harris, M.G., Velakoulis, D., McGorry, P., Pantelis, C., Wood, S.J., 2018. Deterioration of visuospatial associative memory following a first psychotic episode: a long-term follow-up study. Psychol. Med. 48 (1), 132–141.
Wannan, C.M.J., Cropley, V.L., Chakravarty, M.M., Bousman, C., Ganella, E.P., Bruggemann, J.M., Weickert, T.W., Weickert, C.S., Everall, I., McGorry, P., Velakoulis, D., Wood, S.J., Bartholomeusz, C.F., Pantelis, C., Zalesky, A., 2019. Evidence for network-based cortical thickness reductions in schizophrenia. Am. J. Psychiatry 176 (7), 552–563.
Xu, L., 2003. Covariate adjustment in partial least squares for the extraction of the spatial-temporal pattern from positron emission tomography data. University of Pittsburgh.